

Anna Yu. Klikunova<sup>1</sup>, Alexandr V. Khoperskov<sup>2</sup>

DOI: 10.35595/2414-9179-2025-2-31-287-300

## DIGITAL HYDROLOGICAL LANDSCAPE MODEL FOR HYDROLOGICAL SIMULATIONS OF THE RIVER BASIN

### ABSTRACT

Mathematical modeling methods are actively used to analyze hydrological regimes of both water bodies on the Earth's surface and groundwater, sediment transport, and the spread of pollutants. The corresponding numerical models are implemented as software for high-performance computing on multi-GPU and require the specification of a large number of geographically referenced distributions of physical characteristics of the studied area. These data consist of sets of spatial matrices and form the Digital Hydrological Landscape Model (DHLM), the description of which is the main goal of this paper. We distinguish five main DHLM modules, including spatial distributions of parameters necessary for simulating the dynamics of surface and ground water together with sediments. The first module contains spatial matrices of elevations, roughness coefficient of the underlying surface, water sources and sinks, meteorological data, characteristics of hydraulic structures and a number of others. The second and third modules are associated with models of transport of tractional and suspended sediments, respectively. The dynamics of the two types of sediments depends on the characteristics of the water flow and, in turn, affects the topography of the area. This ensures a self-consistent nature of the movement of water and solid particles. The fourth module is designed to support groundwater modeling and contains spatial matrices characterizing the aquifer, soil properties at different depths, and the interaction between surface and underground flows. The fifth module allows processing and visualizing the results of simulations at different points in time against the background of input thematic maps for each of the parameters of the digital hydrological landscape model. Construction of all spatial characteristics of DHLM involves the use of iterative procedures for their consistent refinement. The process of updating the digital elevation model using fusion of elevation data from different sources is discussed in more detail.

**KEYWORDS:** hydrology, sediment transport, digital models, hydrological landscape, computational fluid dynamics

### INTRODUCTION

Computational hydrological models of river systems seem to be an effective tool for analyzing the water state of large natural areas [Khrapov, Khoperskov, 2020; Isaeva et al., 2022; Khrapov, 2023; Lazzarin et al., 2023; Liu et al., 2025]. The quality of such models allows their use as a basis for conducting technical or environmental assessments of various engineering projects, constructing cadastral maps, studying the development features and consequences of emergency events [Agafonnikova, 2017; Pasculli, 2021; Isaeva, Voronin, 2024; Vasil'eva, Belikov, 2024; Sharma, 2025].

Quantitative characteristics of elevation data when creating a digital elevation model (DEM) are a key factor influencing the accuracy of the hydrological regime forecast for a specific

<sup>1</sup> Volgograd State University, Institute of Mathematics and Information Technologies, 100, Universitetsky ave., Volgograd, 400062, Russia, e-mail: [klikunova@volsu.ru](mailto:klikunova@volsu.ru)

<sup>2</sup> Volgograd State University, Institute of Mathematics and Information Technologies, 100, Universitetsky ave., Volgograd, 400062, Russia, e-mail: [khoperskov@volsu.ru](mailto:khoperskov@volsu.ru)

area [Gartsman, Shekman, 2016; Talchabhadel et al., 2021; Okolie, Smit, 2022; Szypula, 2024; Yu et al., 2025; Zhao et al., 2025]. This seems natural, since the elevation matrix  $b_{x_i, y_i}$  is an integral part of the hydrological model. The situation is significantly complicated when long-term forecasts are studied and the relief morphology changes over long periods of time, which leads to a time dependence of the function  $b(x, y, t)$ .

DEM is not the only spatial characteristic that significantly affects the hydrological state of a region. Modern mathematical models of surface water dynamics include a large number of geographically referenced data of relief, soil properties at different depths, groundwater, which form the hydrological regime [Winter, 1999; Khrapov, Khoperskov, 2020; Huggins, 2024; Gebru, 2025;]. Many meteorological and climatic factors also affect land hydrology at different time scales [Winter, 2001; Ye et al., 2018; Isaeva et al., 2022; West et al., 2022; Huggins et al., 2024]. All these parameters can change over time, which significantly complicates the method of quantitative description of the landscape. Various types of hydraulic structures can have a rather complex operating mode. Simple examples can be hydrographs of river dams  $Q(r, t)$  or pumps that provide a given rate of water flow into canals  $q(t)$ . The roughness of the earth's surface changes due to seasonal variability of the vegetation cover. Thus, there is a set of spatial matrices of physical characteristics  $\mathcal{L}$  with possible temporal variability, which determine the mathematical model of hydrological forecasting.

Winter [2001] proposed to study geographical objects as fundamental hydrological landscape units consisting of terrain, geological structure and climatic conditions. This approach allows to simplify the analysis of the interactions of surface, ground and atmospheric waters. The concept of Hydrological Landscape (HL) is intended to provide a conceptualization tool that could be used uniformly regardless of the goals and objectives of the project and the experience of the researchers.

Our work is aimed at developing the concept of the Digital Hydrological Landscape Model (DHLM) as a basis for conducting simulations of the dynamics of hydrological states in a given area. We define the basic structure of DHLM using the example of models for describing the self-consistent dynamics of surface water and groundwater together with traction and suspended sediments. The DHLM consists of a set of geographically referenced spatial matrices. Such a data set specifies quantitative characteristics of the Earth's surface that affect fluid movement.

## RESEARCH MATERIALS AND METHODS

We build on the hydrologic landscape concept of [Winter, 2001], further developed in later studies [West et al., 2022; Huggins et al., 2024; Gebru et al., 2025], and generalize this approach to the large number of physical factors needed for quantitative modeling of hydrologic processes. The basis of the concept of a hydrological landscape is the formation of a landform within a drainage basin. The combined movement of surface and ground waters, sediment transport under specific meteorological and climatic conditions create fundamental hydrological units that interact with each other, inversely influencing the climate system, geochemical and biological processes [Winter, 1999; Kalugin, Lupakov, 2023; Lisina et al., 2025].

The problem of constructing hydrologic landscape maps requires the development of additional tools in conjunction with standard GIS technologies [Winter, 2001]. We attempt to move from the conceptual hydrologic structure [Winter, 2001; Huggins et al., 2024] to the mathematical specification needed for numerical simulations of surface water dynamics. Our efforts are aimed at developing a more rigorous description in the form of a mathematical spatial model of a specific geographic area. Each physical property of the Earth's surface can be characterized by a set of some parameters  $\omega(\ell)$ , which almost always depend on the coordinates  $(x, y)$  and often on time  $t$ . The choice of grid  $\{x_i; y_i\}$  ( $i = 1, \dots, N_x; j = 1, \dots, N_y$  with a step  $\Delta x = \Delta y = \text{const}$ ) is dictated by the DEM resolution and the used basis in the form of initial altitude matrices

of radar topographic survey (SRTM, ASTER, TerraSAR-X/TanDEM-X, GMTED2010, NOAA GLOBE Project, ICESat-2/ATLAS, etc.) [Amra et al., 2025; Zhao et al., 2025], or the results of local projects based on UAV survey [Talchabhadel et al., 2021]. Each such matrix for the value  $\omega(\ell)$  is the  $\ell$ -th thematic map or a subset of thematic layers  $\omega^{(\ell)t_n}$  ( $n = 1, 2, \dots, N_t$ ) in the case of temporary changes in the parameter  $\omega^{(\ell)}$ .

The tuple  $\mathcal{L}$  significantly depends on the choice of a mathematical model for simulating the hydrological state of the study area. We rely on the EcoGIS-Simulation software, which was used to solve a wide range of problems [Khrapov, Khoperskov, 2020; Isaeva et al., 2022; Khrapov, 2023; Khoperskov et al., 2024]. Fig. 1 shows the general structure of the modeling system, where the DHLM consists of four modules in accordance with the four EcoGIS-Simulation computing cores for calculating the dynamics of:

- shallow water,
- traction sediments,
- suspended sediments,
- groundwater.

Moreover, it is possible to consider various combinations of the four modules in the EcoGIS-Simulation software (Fig. 1).

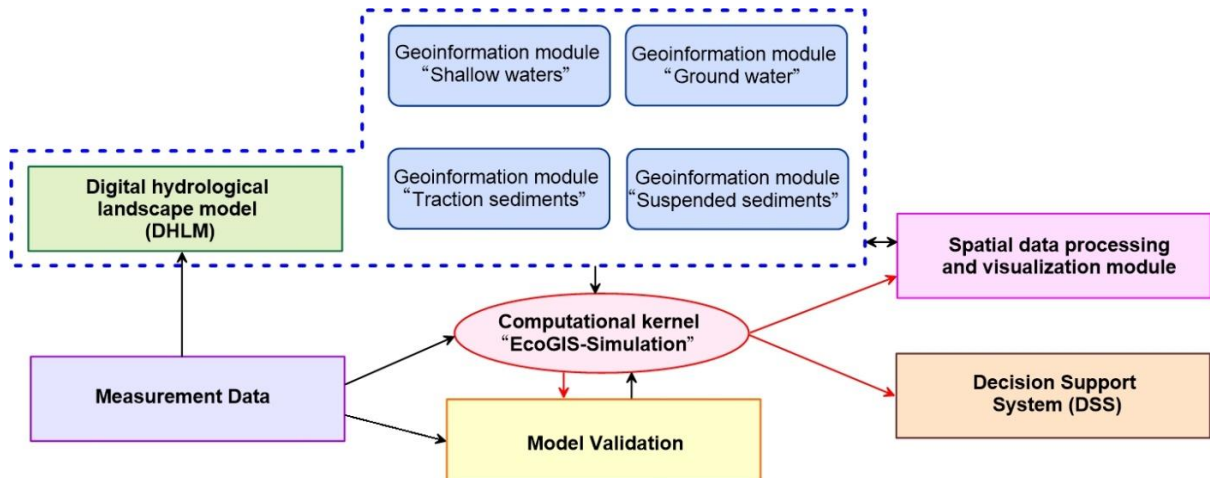


Fig. 1. Main modules of EcoGIS-Simulation software

The initial state of the DHLM is determined by the tuple at time  $t = 0$ , here (1):

$$\mathcal{L}^{(0)} = \langle \omega^{(1)}, \omega^{(2)}, \dots, \omega^{(\ell)}, \dots \omega^{(L)} \rangle_{|t=0} \quad (1).$$

Some parameters in  $\mathcal{H}$  can change significantly during the simulation, such as water sources (hydrographs), roughness coefficient  $n_M$ , wind regime  $\mathbf{W}$ , precipitation, etc. Then the DHLM at any given time is (2):

$$\mathcal{L}^{(n)} = \langle \omega^{(1)}(t_n), \omega^{(2)}(t_n), \dots, \omega^{(\ell)}(t_n), \dots \omega^{(L)}(t_n) \rangle \quad (2).$$

There is a problem of specifying subsets for non-stationary parameters. The direct method of storing a sequence of thematic layers with distributions of some parameter  $\omega^{(\ell)}(t_n)$  at successive time moments  $t_1, t_2, \dots, t_n, \dots$  is simple to implement. However, this greatly increases the number of thematic layers and the tuple  $\mathcal{L}$  becomes three-dimensional as  $\mathcal{L}_{ijn} = \mathcal{L}(x_i, x_j, t_n)$ .

The required hard disk memory turns out to be excessively large. Another negative factor is the decrease in the efficiency of simulations due to the need to frequently load these data into EcoGIS-Simulation. The volume of the DHLM database can be reduced by specifying analytical approximation dependencies for the functions  $\omega^{(\ell)}(t)$ .

The module for data processing and visualization allows to build thematic maps of spatial-temporal distributions of the studied characteristics of the territory. It is intended for the production of DHLM and visualization of input data, first of all. Using this module at the stage of creating spatial DHLM matrices helps to assess the quality of data and detect artifacts. It is possible to visualize the results of hydrodynamic modeling, displaying the distribution of surface (Fig. 6) and groundwater, sediment dynamics, velocity fields of various physical quantities, to build cross-sections of characteristics along arbitrary lines, etc. (Fig. 5).

The quality of hydrological simulations is determined by the accuracy of the spatial matrices  $\mathcal{L}$ . This relationship can be nonlinear, which is clearly illustrated by the example of a digital elevation model  $b_{i,j} = b(x_i, y_j)$ , which key to surface flow movement and subsequent changes in the topography itself. Infiltration and interaction with groundwater are important. Combining elevation data from different sources becomes an urgent need when constructing DEMs, despite all the complexities of fusion algorithms for heterogeneous data [Yu et al., 2025]. Extended areas can be provided with either topographic or satellite radar data. However, this may be unacceptable due to two factors. First, there is a noticeable initial systematic and random error, which can be large, especially for hilly and mountainous areas. Secondly, satellite and geodetic data become outdated and elevation characteristics need to be updated due to natural changes in the relief. Noticeable changes occur primarily in the bathymetry of river systems due to sediment transport during severe floods. Floodplain zones may additionally be subject to elevation changes due to anthropogenic impacts. The observations history of the Northern part of the Volga-Akhtuba floodplain shows examples of strong local transformations of the relief in the process of urbanization of territories (construction of roads and structures, creation of embankments, agricultural activities, etc.).

A certain generalization of HL is the Landscape Ecological Framework (LEF) of territories or ecological nets in the Western European tradition [Meurk, Swaffield, 2000; Khoroshev, 2020]. LEF includes a wider set of characteristics of a given area in addition to the hydrological ones. This approach is an attempt to build a hierarchical system of natural areas that are ranked according to the degree of their ecological role in maintaining the natural balance. An example of such a study is the work of [Zanozin et al., 2024], in which LEF is studied for the Volga River Delta. The landscape-ecological structure of one region of South Africa indicates a significant impact of extreme flooding on the nature of vegetation, demonstrating a change in the trajectory of ecological evolution [Parsons et al., 2005].

## RESEARCH RESULTS AND DISCUSSION

The EcoGIS-Simulation hardware and software package allows modeling both surface [Khrapov, Khoperskov, 2020] and ground waters [Khrapov, 2023], in addition, self-consistent accounting of sediment transport of two types, both suspended and traction ones, is possible. Performing computational experiments requires specifying a large number of input data characterizing the physical properties of the surface, features of the meteorological state of the area, operating modes of hydraulic structures, etc. The Digital Hydrological Landscape Model includes topography and bathymetry as the most important components. In recent years, many researchers have traditionally used data from SRTM radar topographic surveys or other devices. However, such matrices have a large number of artifacts and can produce large errors [Talchabhadel et al., 2021; Okolie et al., 2022; Amra et al., 2025; Zhao et al., 2025], which affects the final results of

water dynamics modeling. In addition, the problem is the construction of a detailed river bottom relief model, since SRTM matrices do not contain bathymetry.

The proposed concept of DHLM is based on the construction of a geographically referenced set of spatial matrices, each of which defines a physical characteristic of the terrain and is used in the EcoGIS-Simulation software. DHLM also includes sets of internal data necessary for the modeling, in addition to the spatial matrices.

Fig. 2 shows the general structure of DHLM in accordance with the division of EcoGIS-Simulation into 4 modules in Fig. 1. The central part of DHLM is the digital elevation model (Fig. 2). The construction of the DEM requires the use of an iterative process, which involves the sequential construction of versions of the spatial matrices of the elevations of a given area  $b_{ij}^{[k]} \rightarrow b_{ij}^{[k+1]}$  ( $k = 0, 1, 2, \dots$ ), which is reflected by the cycle in Fig. 2. The initial DEM matrix  $b_{ij}^{[0]}$  is based on radar topographic survey data using images from the Resurs P and Kanopus B spacecraft.

The base DEM  $b_{ij}^{[0]}$  is supplemented with vectorized data from topographic maps and the results of geodetic surveys at the next stage to clarify the location of water bodies and detect possible errors. Relief changes can also be caused by anthropogenic factors (yellow block in Fig. 2). These include works to protect settlements and roads as floodplain zones become urbanized (diversion ditches and embankments), related to clearing riverbeds, state projects to improve water supply to the territory, and melioration works. Such DEM updating should be carried out on a regular basis.

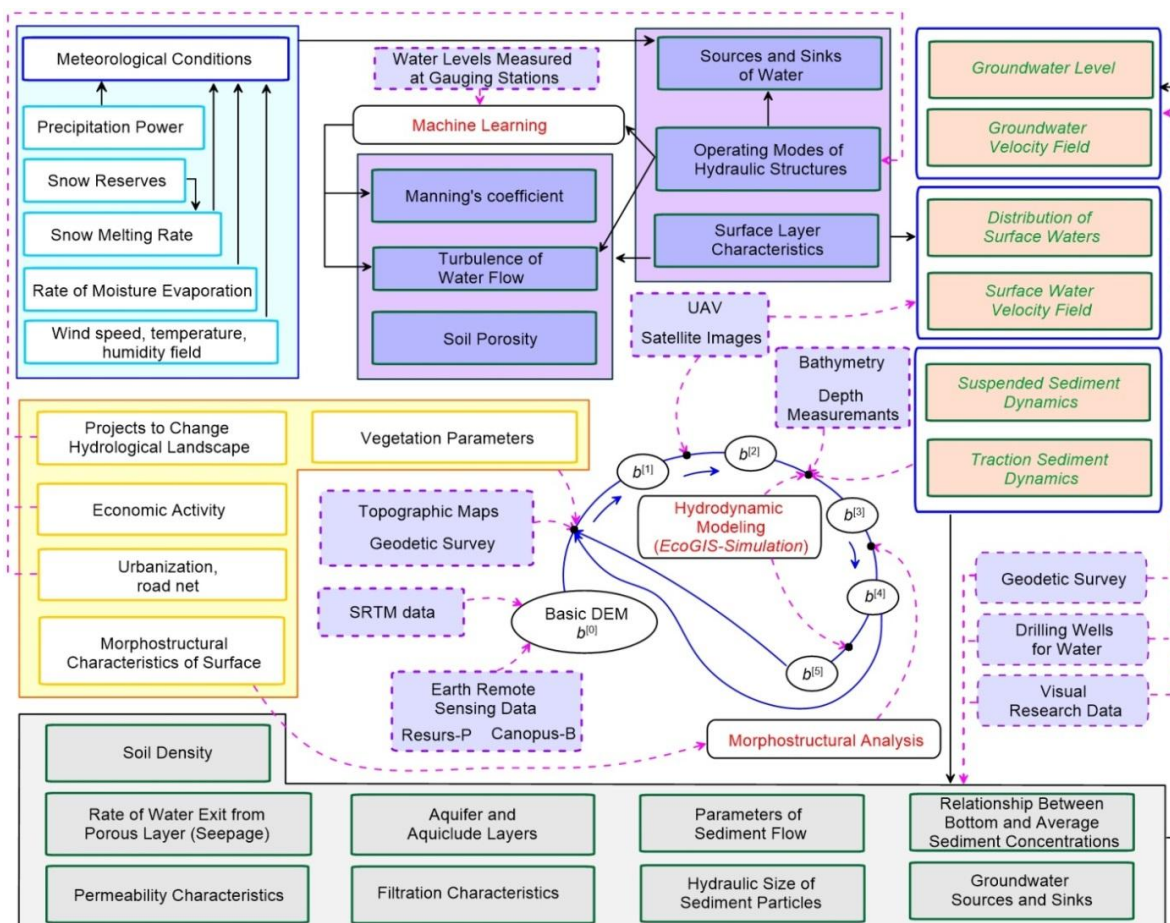


Fig. 2. Structure of the digital hydrological landscape model

The next step involves updating the DEM using data on transient water bodies with rapidly changing boundaries, which is typical for periodically flooded floodplain areas. Data on the location of the shorelines of such water bodies allow supplementing the existing  $b_{ij}^{[2]}$  matrices with lines of constant elevations. The sources for this are measurements from unmanned aerial vehicles and series of space images at different points in time. It should also be noted that space imagery and UAV data can also be used to construct the spatial distribution of surface waters during hydrodynamic modeling. Such information can be both an input data set for the initial conditions of modeling and used to verify the modeling results when comparing the obtained flood maps with real data.

Further transformation of matrices  $b_{ij}^{[2]} \rightarrow b_{ij}^{[3]}$  consists in constructing a digital relief of the bottom of water bodies. The methods for constructing such a model are similar to those used in constructing land surface elevation matrices and consist in transforming vector depth data into spatial elevation matrices using interpolation algorithms. An important part of the work at this stage is determining the hydrological connection between all water bodies in the region [Klikunova, Khoperskov, 2023]. Bathymetry usually changes faster than land relief due to the dynamics of suspended and traction sediments in the conditions of a non-stationary hydrograph. Therefore, updating methods using hydrodynamic simulations of sediment transport give good results [Khrapov, 2023].

The matrix  $b_{ij}^{[3]}$  can already be used to conduct computational experiments. Since they require large computational and time resources, another stage of updating the DEM  $b_{ij}^{[3]} \rightarrow b_{ij}^{[4]}$  is useful, using the morphostructural analysis of the relief surface [Erunova, Yakubailik, 2024]. Such a study of the matrix  $b_{ij}$  allows us to determine various geometric characteristics of the surface (angles, curvature, steps, cliffs, saddles, peaks, channel structures, etc.). Geoinformation modeling of water flow movement in the geoinformation system QGIS requires fewer resources compared to numerical hydrodynamic experiments, allowing us to detect remaining artifacts.

A satisfactory result of the morphostructural analysis allows us to proceed to hydrodynamic modeling using the EcoGIS-Simulation software [Khrapov, Khoperskov, 2020]. The diagram in Fig. 2 highlights hydrodynamic modeling only as an intermediate stage for verifying DEM  $b_{ij}^{[4]}$ . However, this process is quite complex and requires a large number of iterations. For example, the procedure for constructing an adequate hydraulic resistance model for a section of the Volga River in [Khoperskov et al., 2024] required 32 experiments and neural network modeling. The described process is iterative and involves multiple changes and additions to the obtained matrices if necessary.

Our iterative approach to constructing DEM is necessary for high-fidelity hydrodynamic simulations. Since the traditionally used SRTM matrices give too large elevation errors. The original SRTM matrix does not include the river bathymetry and there are significant discrepancies near the coastlines. The comparison of elevation data in our third iteration  $b_{ij}^{[3]}$  is carried out with the Shuttle Radar Topography Mission with a cell size of  $30 \times 30$  m. Matching the matrices requires transforming the SRTM to a grid with a given step  $\Delta x$ . The first stage of the algorithm is based on constructing a system of vector isolines (contours) of elevations using standard GIS “Panorama” tools. The step of the isolines allows you to control the errors when calculating the new matrix. Then, the constructed vector map is used to calculate the elevations  $b_{ij}^{(SRTM)}$  on a grid with a step of  $\Delta x$ . Fig. 3 shows an example of calculating the difference  $b_{ij}^{[3]} - b_{ij}^{(SRTM)}$  for a DEM with  $\Delta x = 5$  m covering a section of the Medveditsa River near the city of Zhirnovsk in the Volgograd

Region. Since we use  $b_{ij}^{[3]}$ , the differences are clearly visible only in the river zone and its immediate surroundings.

Surface water dynamics is determined not only by DEM, but also by the properties of the underlying surface. The key parameter is the Manning roughness coefficient  $n_M$ , which affects the hydraulic resistance to flow. The value of  $n_M$  depends on the type of vegetation, which can significantly change the velocity and direction of water flow at small depths, so the construction of a spatial distribution matrix of the roughness coefficient is based on identifying areas with different types and densities of vegetation (Fig. 4). The parameter  $n_M$  also depends on the type of soil. For example, the roughness coefficient of sand is only 0.02, and  $n_M$  for arable land can reach 0.05.

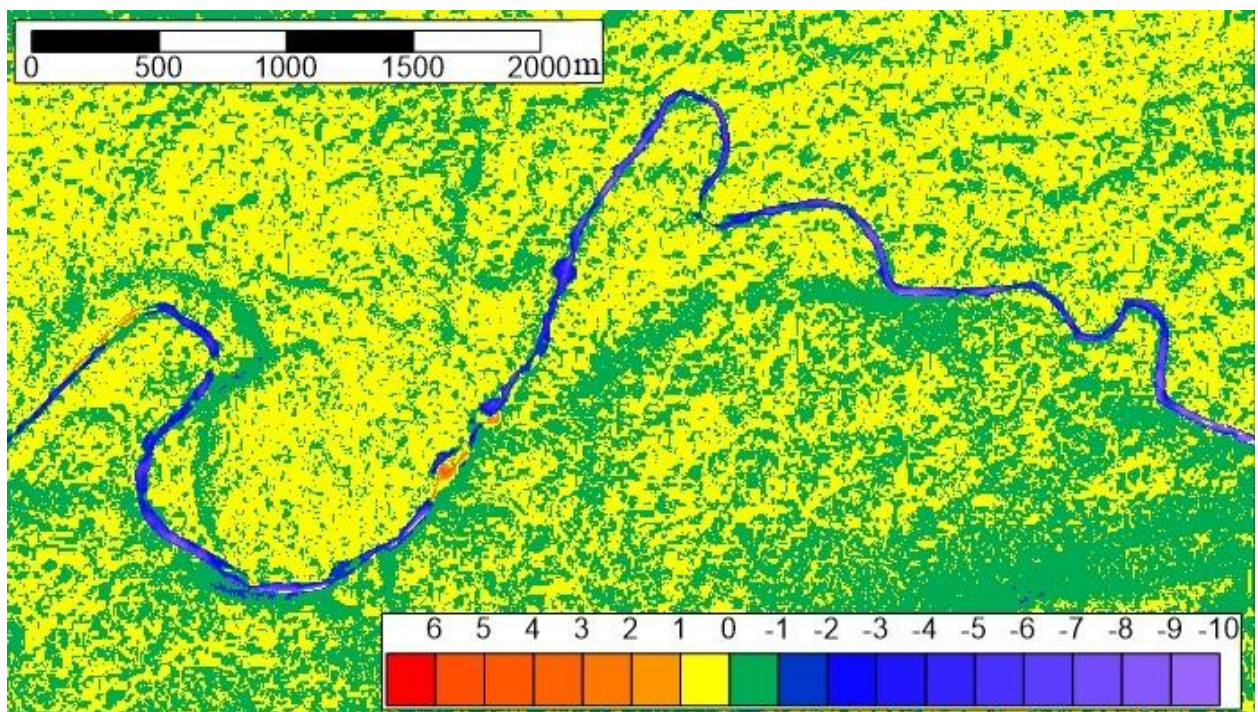


Fig. 3. Difference between DEM  $b_{ij}^{[3]}$  and matrix  $b_{ij}^{(SRTM)}$  for 5-meter grid

Determining the  $n_M$  coefficient for a large river channel is a complex task, since it requires a detailed analysis of the river channel characteristics, including the influence of bedforms of different sizes, the shape of the river channel cross-section, fluid flow non-stationarity, channel slope, aquatic vegetation, and other factors [Das, Khatua, 2018]. The  $n_M$  values can vary significantly in different river systems [Coon, 1998; Xia et al., 2012; Hatzigiannakis et al., 2016; Ye et al., 2018]. To determine the value of the roughness coefficient of the Volga River bed, we proposed a method for restoring this parameter using machine learning, which can be applied to other rivers as well [Klikunova et al., 2023; Khoperskov et al., 2024].

Modeling groundwater dynamics requires spatial matrices with the properties of the aquifer (Fig. 5). For example, the soil porosity  $\psi$  defines the pore volume per unit volume of soil [Khrapov, 2023] and  $\psi = 1 - \gamma_s$ , where  $\gamma_s = \varrho_a / \varrho_s$  is the relative volume of solids per unit volume of soil,  $\varrho_s$  is the density of solids,  $\varrho_d$  is the density of the skeleton (dry) soil. The dynamics equations also contain the porosity coefficient  $k_p = \psi / (1 - \psi)$ . The groundwater level is defined by  $\eta_g(x, y, t) = H_g(x, y, t) + b_g(x, y)$ , where  $H_g(x, y, t)$  is the thickness of the groundwater layer above the low-permeability soil relief  $b_g(x, y)$ . Effective measuring devices are available for

constructing the aquifer  $b_g(x, y)$ . Fig. 5 shows the profiles of various characteristics along the line  $AB$  marked in Fig. 6.

The next DHLM block includes a set of characteristics for modeling sediment dynamics. These parameters define complex processes of erosion and sedimentation of solid particles in water, described within the framework of the so-called subgrid physics. The main coefficients include [Khrapov, Khoperskov, 2020; Khrapov, 2023]:

1.  $q_{ba}$  is the rate of flux of the bottom soil due to gravitational settling of suspended sediments;
2. the coefficients  $a_j$  and  $m_j$  determine the properties of the transported material [Li et al., 2017; Hafiyana et al., 2021; Ndengna, Njifenjou, 2022];
3. the critical velocity  $u^{(cr)}$  ensures the onset of bottom erosion [Shao, Wang, 2005];
4. the empirical constant  $c_v$  characterizes the cohesion of traction sediments and depends on the type and condition of the soil [Venditti et al., 2005];
5. mass density of river sediment material  $\rho_s$ ;
6. median particle size of river sediments  $d_{50}$ ;
7. density of bottom sediment soil  $\rho_g = (1 - \psi)\rho_s$ ;
8.  $\bar{\rho}_*$  is the averaged over the depth of the flow  $H$  suspended sediment density (turbidity);
9.  $q_\alpha$  is the rate of suspended sediment influx;
10.  $D$  is the integral diffusion coefficient of suspended sediments in the horizontal direction;
11. hydraulic particle size of sediment particles  $w$ ;
12. coefficient of connection between bottom and average depth sediment concentrations  $\varphi_\alpha$ ;
13.  $\nu_0$  is the coefficient of kinematic viscosity of water, which depends on temperature.

We must also specify the distributions of water sources and sinks in the computational domain. The operating mode of hydraulic structures provides such data through special sensors. However, there are natural sources and sinks, the determination of which is difficult and requires additional model assumptions. Water balance  $q = q^{(s)} - q^{(inf)} - q^{(ev)} + q_g^{(up)}$  determines the rate of fluid inflow/outflow under the influence of various factors, where  $q^{(s)}(x, y, t)$  is the rate of water inflow through hydraulic structures and due to precipitation,  $q^{(inf)}(x, y, t)$  is the function of runoff due to seepage (infiltration) into the ground,  $q^{(ev)}$  is the rate of water loss due to evaporation,  $q_g^{(up)}$  is the rate of seepage (rise) of groundwater to the surface.

One of the DHLM modules provides work with meteorological data, including precipitation, snow reserves, wind and temperature conditions, etc. Fig. 7 demonstrates the effect of meteorological conditions on the water level in the Volga River below the Volga Hydroelectric Power Station. The dam hydrograph  $Q(t)$  determines the annual water charge from the Volgograd Reservoir. This hydrograph, as a rule, completely controls the flow in the channels of the Volga, Akhtuba and small floodplain channels (Fig. 6). The consistent behavior of the time dependencies  $Q(t)$  and  $\eta(t)$  after the 100th day is clearly visible, both for the flood stage ( $t = 100 - 175$  days) and during the low-water period ( $t > 175$  days). The green line in Fig. 7 shows the imbalance at the beginning of the year ( $t < 80$ ), when there is a nearly two-meter rise in water level that is not related to the discharge through the dam. The hydrograph changes little during the first 100 days, so the increase  $\eta(t < 100$  days) is caused by another reason. Thus, the additional water discharge is due to other water sources associated with the inflow in addition to the dam. The computational model must reproduce these features, which requires specifying water sources  $q^{(s)}$  through small tributaries along the Volga channel.

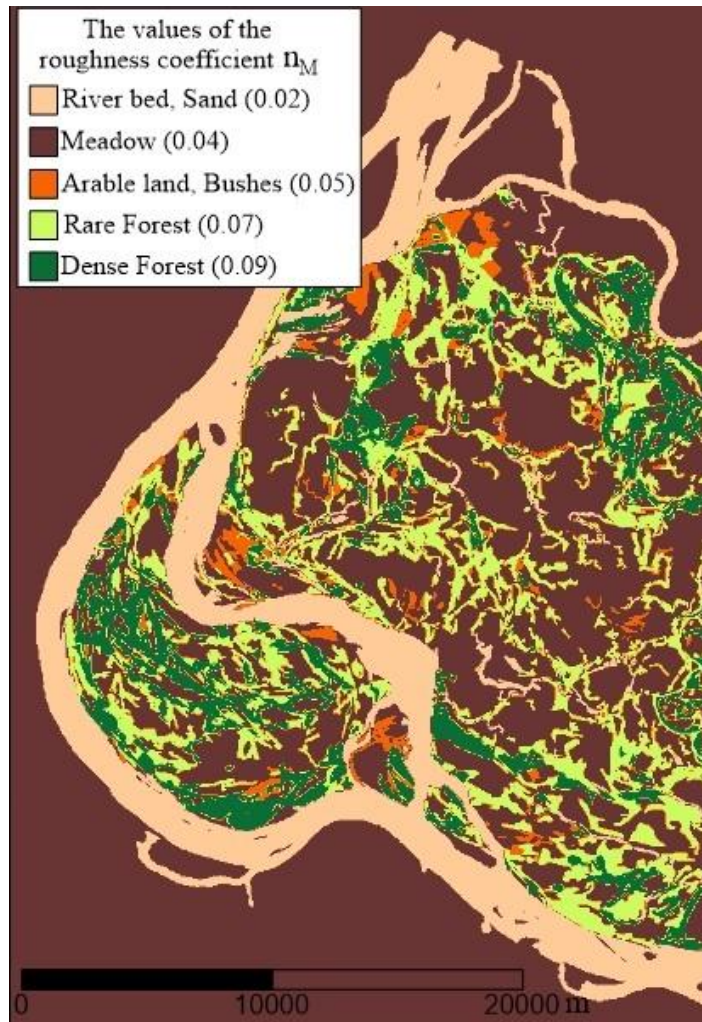


Fig. 4. Distribution of the coefficient  $n_M$  for the fragment of computational domain of the northern part of the Volga-Akhtuba floodplain

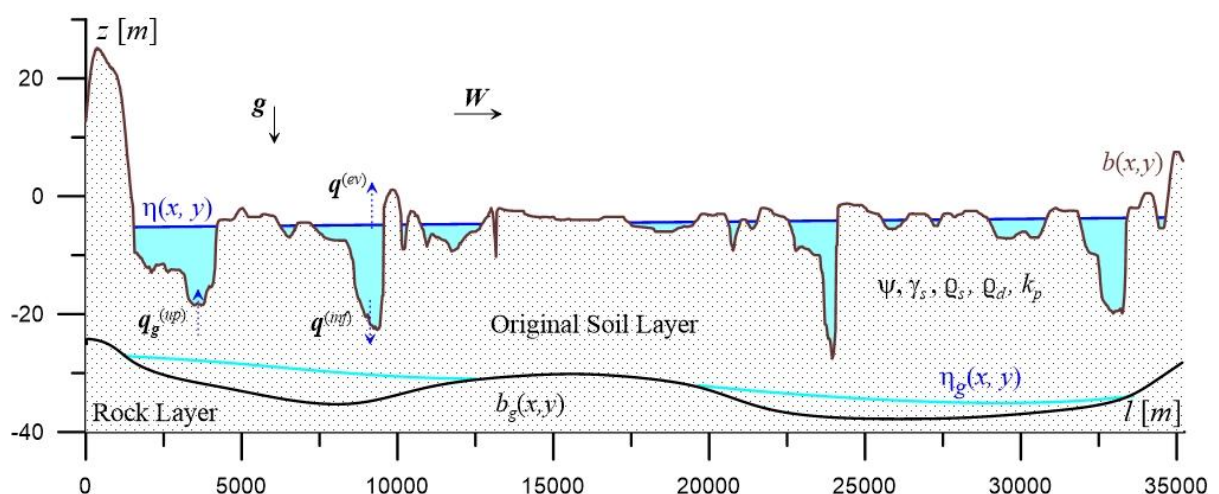


Fig. 5. An example of the distribution of surface and ground water, relief profiles  $b(x,y)$  and the boundary  $b_g(x,y)$  between porous soil (sand, loam, etc.) and low-permeability soil (clay, silt, etc.)

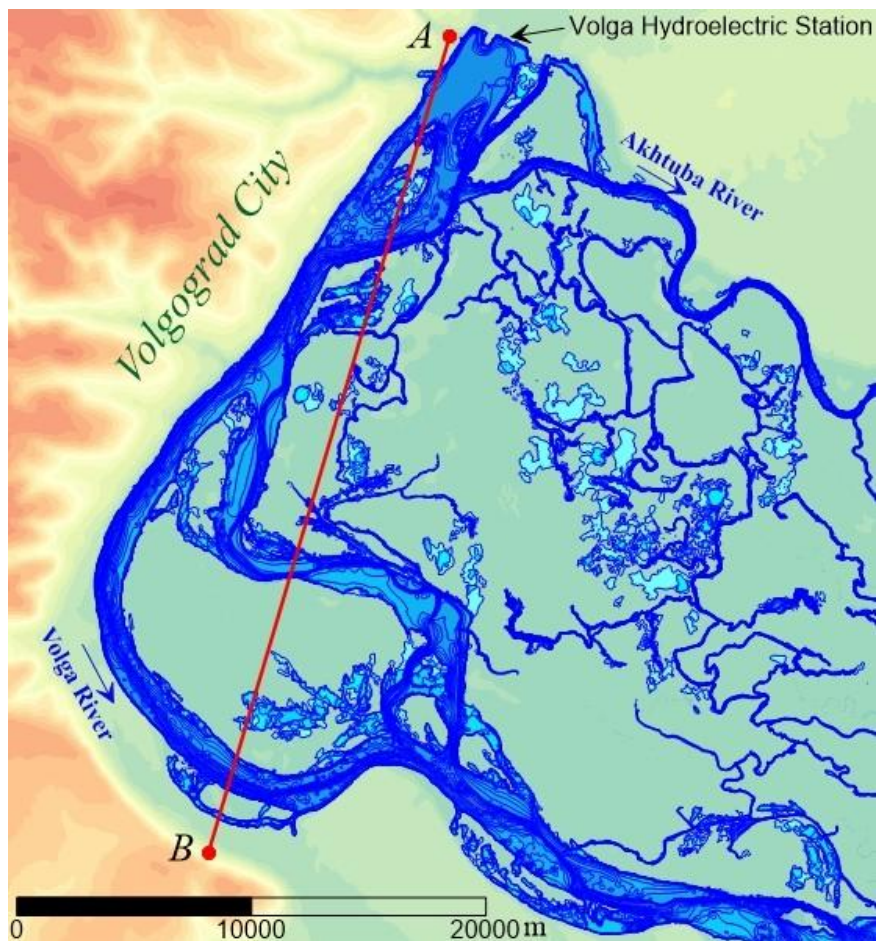


Fig. 6. Digital model of the northern part of the interflue of the Volga and Akhtuba Rivers with superimposed water distribution in the hydrodynamic model

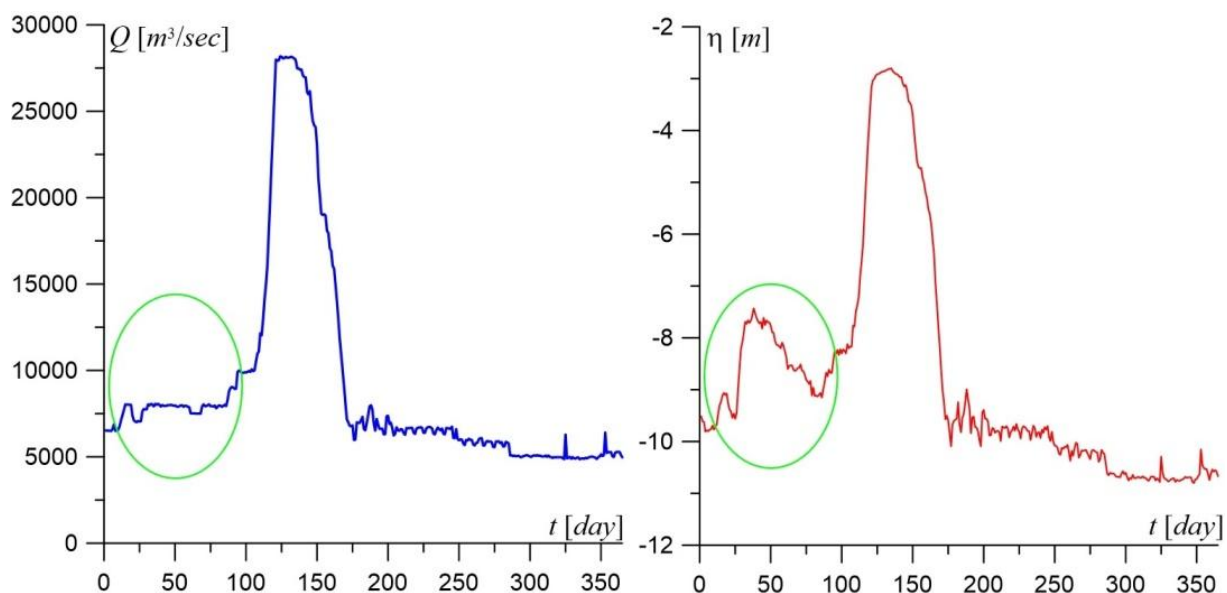


Fig. 7. Left — Hydrograph of the Volga hydroelectric power station in 2005.  
Right — Corresponding behavior of the water level in the Dam Downstream

## CONCLUSIONS

Mathematical modeling methods for studying hydrological regimes of complex river systems require specifying a large number of characteristics, which are generally heterogeneous and can change over time. We are developing an approach for generating input spatial data that determine the conditions for conducting computational experiments for river system hydrology problems in a multicomponent model for the EcoGIS-Simulation software in the form of a digital hydrological landscape model. A basic version of DHLM has been created for the Northern part of the Volga-Akhtuba floodplain and some other water bodies in the form of sets of georeferenced thematic layers for data processing in a specialized geographic information system. It is important to note that the spatial matrices  $\omega^{(\ell)}$  should be iteratively refined as more accurate and relevant data becomes available. As an initial basic distribution, one can limit oneself to specifying a constant corresponding to the average typical value for the study area.

We describe in more detail an iterative method for constructing a digital elevation model that provides fusion of heterogeneous spatial data into a single up-to-date DEM. The use of hydrodynamic simulations appears to be a powerful tool for the procedure of refining the DEM by comparing with observational data.

DHLM also has a large independent research potential in addition to its use in numerical hydrodynamic experiments. Our approach enables quantitative comparison of hydrological landscape units with each other to identify both common properties and to find significantly different (unlike) structures in the original concept of the hydrological landscape in the work [Winter, 2001]. This method seems promising especially due to the availability of a large number of new tools for intelligent analysis of multidimensional data. DHLMs can also provide new quantitative results in constructing a landscape-ecological framework of territories [Meurk, Swaffield, 2000], going beyond the cartographic approach.

## ACKNOWLEDGEMENTS

This work supported by the Russian Science Foundation (grant No. 23-71-00016, <https://rscf.ru/project/23-71-00016/>). The research also relied on the shared research facilities of the HPC computing resources at Lomonosov Moscow State University.

## REFERENCES

Agafonnikova E. O., Klikunova A. Yu., Khoperskov A. V. Computer Simulation of the Volga River Hydrological Regime: Problem of Water-Retaining Dam Optimal Location. Bulletin of the South Ural State University, Series: Mathematical Modelling, Programming and Computer Software, 2017. V. 10. No. 3. P. 148–155. DOI: 10.14529/mmp170313.

Amra R., Araki S., Geib C., Davies G. Error-Reduced Digital Elevation Models and High-Resolution Land Cover Roughness in Mapping Tsunami Exposure for Low Elevation Coastal Zones. Remote Sensing Applications: Society and Environment, 2025. V. 37. P. 101438. DOI: 10.1016/j.rsase.2024.101438.

Coon W. F. Estimation of Roughness Coefficients for Natural Stream Channels with Vegetated Banks. US Geological Survey Water-Supply Paper, 1998. V. 2441. P. 133.

Das B. S., Khatua K. K. Flow Resistance in a Compound Channel with Diverging and Converging Floodplains. Journal of Hydraulic Engineering, 2018. V. 144. No. 8. P. 04018051. DOI: 10.1061/(ASCE)HY.1943-7900.0001496.

Erunova M. G., Yakubailik O. E. Geomorphometric Analysis of Agricultural Areas Based on the FABDEM Digital Elevation Model. InterCarto. InterGIS, 2024. V. 30. Part 2. P. 252–262. DOI: 10.35595/2414-9179-2024-2-30-252-262.

*Gartsman B. I., Shekman E. A.* Potential of River Network Modeling Based on GIS Technologies and Digital Elevation Model. *Russian Meteorology and Hydrology*, 2016. V. 41. No. 1. P. 63–71. DOI: 10.3103/S1068373916010088.

*Gebru H., Gebreyohannes T., Hagos E., Perilli N.* Hydrogeological Assessment and Steady-State Groundwater Flow Modeling for Groundwater Management in the Golina River Sub-Basin, Northern Ethiopia, Using MODFLOW 6. *Water*, 2025. V. 17. No. 7. P. 949. DOI: 10.3390/w17070949.

*Hafiyana Q., Harlanb D., Adityawanb M. B., Natakusumahc D. K., Magdalena I.* 2D Numerical Model of Sediment Transport Under Dam-break Flow Using Finite Element. *International Journal on Advanced Science, Engineering and Information Technology*, 2021. V. 11. No. 6. P. 2476–2481.

*Hatziyiannakis E., Pantelakis D., Hatzispiroglou I., Arampatzis G., Ilias A., Panagopoulos A.* Discharge Measurements and Roughness Coefficient Estimation in a River. The Case of Strymonas River in Northern Greece. *Environmental Processes*, 2016. V. 3. No. 1. P. 263–275. DOI: 10.10107/s40710-015-0120-4.

*Huggins X., Gleeson T., Villholth K. G., Rocha J. C., Famiglietti J. S.* Groundwaterscapes: A Global Classification and Mapping of Groundwater's Large-Scale Socioeconomic, Ecological, and Earth System Functions. *Water Resources Research*, 2024. V. 60. No. 10. P. e2023WR036287. DOI: 10.1029/2023WR036287.

*Isaeva I. I., Voronin A. A.* Models for Managing Hydraulic Projects in Floodplain Areas, Considering the Activity of Economic Entities. *Mathematical physics and computer simulation*, 2024. V. 27. No. 1. P. 45–61 (in Russian). DOI: 10.15688/mpcm.jvolsu.2024.1.4.

*Isaeva I. I., Voronin A. A., Khoperskov A. V., Kharitonov M. A.* Modeling the Territorial Structure Dynamics of the Northern Part of the Volga-Akhtuba Floodplain. *Computation*, 2022. V. 10. No. 4. P. 62. DOI: 10.3390/computation10040062.

*Kalugin A. S., Lupakov S. Yu.* The Effect of Natural and Anthropogenic Climate Changes on River Runoff and Snow Water Equivalent in the Lena River Basin. *Water Resources*, 2023. V. 50. No. 4. P. 557–568 (in Russian). DOI: 10.1134/S0097807823040139.

*Khoperskov A. V., Khrapov S. S., Klikunova A. Yu., Popov I. E.* Efficiency of Using GPUs for Reconstructing the Hydraulic Resistance in River Systems Based on Combination of High Performance Hydrodynamic Simulation and Machine Learning. *Lobachevsky Journal of Mathematics*, 2024. V. 45. No. 7. P. 3085–3096. DOI: 10.1134/S199508022460376X.

*Khoroshev A.* Landscape-Ecological Approach to Spatial Planning as a Tool to Minimize Socio-Ecological Conflicts: Case Study of Agrolandscape in the Taiga Zone of Russia. *Land*, 2020. V. 9. No. 6. P. 192. DOI: 10.3390/land9060192.

*Khrapov S. S.* Numerical Modeling of Hydrodynamic Accidents: Erosion of Dams and Flooding of Territories. *Vestnik of St. Petersburg University, Mathematics*, 2023. V. 56. No. 2. P. 261–272. DOI: 10.1134/S1063454123020085.

*Khrapov S. S., Khoperskov A. V.* Application of Graphics Processing Units for Self-Consistent Modelling of Shallow Water Dynamics and Sediment Transport. *Lobachevsky Journal of Mathematics*, 2020. V. 41. No. 8. P. 1475–1484. DOI: 10.1134/S1995080220080089.

*Klikunova A. Yu., Khoperskov A. V.* Calculation of Hydrological Connection Between the Volga River and the Akhtuba River Using Numerical Hydrodynamic Modeling. *St. Petersburg State Polytechnical University Journal. Physics and Mathematics*, 2023. V. 16. No. 1. P. 326–330. DOI: 10.13140/RG.2.2.24361.67683.

*Klikunova A. Yu., Polyakov M. V., Khrapov S. S., Khoperskov A. V.* Problem of Building High-Quality Predictive Model of River Hydrology: The Combined Use of Hydrodynamic Simulations and Intelligent Computing. *Communications in Computer and Information Science*, 2023. V. 1909. P. 191. DOI: 10107/978.-3-031-44615-3\_13.

*Lazzarin T., Defina A., Viero D. P.* Assessing 40 Years of Flood Risk Evolution at the Micro-Scale Using an Innovative Modeling Approach: The Effects of Urbanization and Land Planning. *Geosciences*, 2023. V. 13. No. 4. P. 112. DOI: 10.3390/geosciences13040112.

*Li W., Hu P., Pähzt T., He Z., Cao Z.* Limitations of Empirical Sediment Transport Formulas for Shallow Water and their Consequences for Swash Zone Modelling. *Journal of Hydraulic Research*, 2017. V. 55. No. 1. P. 114–120. DOI: 10.1080/00221686.2016.1212942.

*Lisina A. A., Frolova N. L., Kalugin A. S., Krylenko I. N., Motovilov Yu. G.* Assessment of the Kolyma River Hydrological Regime Dynamics in the 21st Century Based on Runoff Formation Model. *Geography, Environment, Sustainability*, 2025. V. 18. No. 1. P. 23–34. DOI: 10.24057/2071-9388-2025-3482.

*Liu T., Trim S. J., Ko S. B., Spiteri R. J.* The Multi-GPU Wetland DEM Ponding Model. *Computers & Geosciences*, 2025. V. 199. P. 105912. DOI: 10.1016/j.cageo.2025.105912.

*Meurk C. D., Swaffield S. R.* A Landscape Ecological Framework for Indigenous Regeneration in Rural New Zealand-Aotearoa. *Landscape and Urban Planning*, 2000. V. 50. Iss. 1–3. P. 129–144. DOI: 10.1016/S0169-2046(00)00085-2.

*Ndengna A. R. N., Njifenjou A.* A Well-Balanced PCCU-AENO Scheme for a Sediment Transport Model. *Ocean Systems Engineering*, 2022. V. 12. No. 3. P. 359–384. DOI: 10.12989/ose.2022.12.3.359.

*Okolie C. J., Smit J. L.* A Systematic Review and Meta-Analysis of Digital Elevation Model (DEM) Fusion: Pre-processing, Methods and Applications. *ISPRS Journal of Photogrammetry and Remote Sensing*, 2022. V. 188. P. 1–29. DOI: 10.1016/j.isprsjprs.2022.03.016.

*Parsons M., McLoughlin C. A., Kotschy K. A., Rogers K. H., Rountree M. W.* The Effects of Extreme Floods on the Biophysical Heterogeneity of River Landscapes. *Frontiers in Ecology and The Environment*, 2005. V. 3. Iss. 9. P. 487–494. DOI: 10.1890/1540-9295(2005)003[0487:TEOEFO]2.0.CO;2.

*Pasculli A., Cinosi J., Turconi L., Sciarra N., Sciarra N.* Learning Case Study of a Shallow-Water Model to Assess an Early-Warning System for Fast Alpine Muddy-Debris-Flow. *Water*, 2021. V. 13. No. 6. P. 750. DOI: 10.3390/w13060750.

*Shao X. J., Wang X. K.* Introduction to River Mechanics. 2005.

*Sharma A. P., Fu X., Kattel G. R., Adhikari T. R., Hassan M. A.* Appraising Flood Risk and Inundation Extent Using GIS-aided 2D Hydraulic Modeling in Nepal Himalaya: A Case of West Rapti River Basin. *Modeling Earth Systems and Environment*, 2025. V. 11. No. 3. P. 176. DOI: 10.1007/s40808-025-02356-5.

*Szypula B.* Accuracy of UAV-based DEMs without Ground Control Points. *Geoinformatika*, 2024. V. 28. No. 1. P. 1–28. DOI: 10.1007/s10707-023-00498-1.

*Talchabhadel R., Nakagawa H., Kawaike K., Yamanoi K., Thapa B. R.* Assessment of Vertical Accuracy of Open Source 30 m Resolution Space-Borne Digital Elevation Models. *Geomatics, Natural Hazards and Risk*, 2021. V. 12. No. 1. P. 939–960. DOI: 10.1080/19475705.2021.1910575.

*Vasil'eva E. S., Belikov V. V.* Numerical Modeling of a Cascade Hydrodynamic Breakdown at the Verkhneuralsk and Magnitogorsk Dams. Power Technology and Engineering, 2024. V. 57. P. 724–732. DOI: 10.1007/s10749-024-01726-w.

*Venditti J. G., Church M. A., Bennett S. J.* Bed Form Initiation from a Flat Sand Bed. Journal of Geophysical Research: Earth Surface, 2005. V. 110. No. F1. P. 1–19. DOI: 10.1029/2004JF00149.

*West C., Rosolem R., MacDonald A. M., Cuthbert M., Wagener T.* Understanding Process Controls on Groundwater Recharge Variability across Africa through Recharge Landscapes. Journal of Hydrology, 2022. V. 612. P. 127967. DOI: 10.1016/j.jhydrol.2022.127967.

*Winter T. C.* Relation of Streams, Lakes, and Wetlands to Groundwater Flow Systems. Hydrogeology Journal, 1999. V. 7. P. 28–45.

*Winter T. C.* The Concept of Hydrologic Landscapes. Journal of the American Water Resources Association, 2001. V. 37. No. 2. P. 335–349. DOI: 10.1111/j.1752-1688.2001.tb00973.x.

*Xia J., Lin B., Falconer R. A., Wang Y.* Modelling of Man-made Flood Routing in the Lower Yellow River, China. Thomas Telford Ltd.: Proceedings of the Institution of Civil Engineers-Water Management, 2012. V. 165. No. 7. P. 377–391. DOI: 10.1680/wama.11.00028.

*Ye A., Zhou Z., You J., Ma F., Duan Q.* Dynamic Manning's Roughness Coefficients for Hydrological Modelling in Basins. Hydrology Research, 2018. V. 49. No. 5. P. 1379–1395. DOI: 10.2166/nh.2018.175.

*Yu C., Wang Q., Zhang Z., Zhong Z., Ding Y., Lai T., Huang H., Shen P.* Multi-Source Data Joint Processing Framework for DEM Calibration and Fusion. International Journal of Applied Earth Observation and Geoinformation, 2025. V. 139. P. 104484.

*Zanozin V. V., Barmin A. N., Zanozin V. V.* Geospatial Modeling of the Organization of the Landscape-Ecological Framework of the Volga Delta. InterCarto. InterGIS. Moscow: Lomonosov Moscow State University, Faculty of Geography, 2024. V. 30. Part 1. P. 80–93 (in Russian). DOI: 10.35595/2414-9179-2024-1-30-80-93.

*Zhao Y., Wu B., Kong G., Zhang H., Wu J., Yu B., Wu J., Fan H.* Generating High-Resolution DEMs in Mountainous Regions Using ICESat-2/ATLAS Photons. International Journal of Applied Earth Observation and Geoinformation, 2025. V. 138. P. 104461. DOI: 10.1016/j.jag.2025.104461.